JOURNAL OF PHYSICAL ORGANIC CHEMISTRY
J. Phys. Org. Chem. 2007; **20:** 30–43
Published online in Wiley InterScience
(www.interscience.wiley.com) DOI: 10.1002/poc.1122

Host–guest complexes of phenol derivatives with β-cyclodextrin: an experimental and theoretical investigation

Saloua Chelli,[1,2] Mustapha Majdoub,[1] Mohamed Jouini,[2]* Salah Aeiyach,[2] François Maurel,[2] Kathleen I. Chane-Ching[2] and Pierre-Camille Lacaze[2]

[1]Laboratoire des Polymères, Biopolymères et Matériaux Organiques, Faculté des Sciences de Monastir, Boulevard de l'Environnement, 5019 Monastir, Tunisia
[2]Laboratoire Interfaces, Traitements, Organisation et Dynamique des Systèmes, CNRS UMR 7086, Université Paris 7 – Denis Diderot, 1 rue Guy de la Brosse, 75005 Paris, France

Received 8 May 2006; revised 4 July 2006; accepted 20 July 2006

ABSTRACT: β-Cyclodextrin (β-CD) is used as the host molecule to study the inclusion of a series of bent [bisphenol A (BPA) and fluorinated bisphenol A (FBPA)] or linear [biphenol (BIP) and isopropylphenol (IPP)] phenol derivatives. Experimental and theoretical investigations reveal that the complexes with the bent BPA and FBPA molecules are more stable than those with the linear IPP and BIP molecules. This stability difference is attributed to differences in the geometries which, in the case of bent molecules, seems to prevent the unthreading of the guest. The optimized geometry of the BIP/β-CD complex shows a particularly strong deviation of the principal axis of BIP from the vertical symmetry axis (C_7) of β-CD. For bent molecules, the same sort of deviation is due to the second aromatic residue, which is outside the cavity, approaching the wider rim of the β-CD, probably because of van der Waals interactions. In the FBPA/β-CD system, experimental results (^{19}F NMR) and DFT (MPWB1K//AM1) calculations demonstrate a different complexation mode from that of the three other systems, with high interaction energy, the phenol residues are located outside the β-CD cavity but fluorinated alkyls are inside. This agreement indicates that MPWB1K/6-31G(d) single point calculation based on AM1 geometries is a useful predictive tool for such series, even for systems as large as ours. Copyright © 2007 John Wiley & Sons, Ltd.

KEYWORDS: β-cyclodextrin; bisphenol A; host–guest inclusion compounds; AM1; DFT

INTRODUCTION

Over the past two decades, a major research interest in the field of supramolecular chemistry has been the design and synthesis of structures using the molecular recognition of small guest molecules by large hosts.[1] Non-covalent intermolecular interactions are used to synthesize supramolecular assemblies such as rotaxanes, polyrotaxanes, and catenanes.[2–4] A variety of macrocyclic host molecules are able to form inclusion complexes with organic compounds. So far, among these host molecules, cyclodextrins are the most popular and have been employed to form inclusion complexes with a variety of organic compounds in water. Hydrophobic forces are mainly responsible for driving a guest into the cavity.[5] Depending on the nature and the size of guest, several types of host–guest complexes between these organic guests and cyclodextrins with 1/1, 1/2, 2/1, and 2/2 stoichiometries have been observed,[5–7] and many complexes have been used in applications such as pharmaceutics,[8,9] biomimetic chemistry,[10] catalysis,[11] and chemical analysis.[12]

Bisphenol A (BPA) is an important industrial intermediate very widely used to manufacture polycarbonate,[13] polyethers,[14] polyesters,[15] epoxy resins and coatings,[16] polysulfones,[17] and other useful products. Since it is slightly toxic to fish and invertebrate species[18], its concentration in the environment is regularly surveyed and, therefore, new analysis techniques for BPA traces have been proposed. Kitano *et al*. studied the inclusion of bisphenol derivatives with several β-cyclodextrins using 2-anilinonaphthalene-6-sulfonic acid as probe,[19] as well as the inclusion of bisphenols in self-assembled monolayers of thiolated β-cyclodextrin (β-CD) on a gold electrode.[20] Del Olmo *et al*.[21] proposed the use of β-CD inclusion complexes to analyze BPA residues in water by spectrofluorimetric measurements. They reported a

**Correspondence to:* M. Jouini, Laboratoire Interfaces, Traitements, Organisation et Dynamique des Systèmes, CNRS UMR 7086, Université Paris 7 – Denis Diderot, 1 rue Guy de la Brosse, 75005 Paris, France.
E-mail: jouini@paris7.jussieu.fr

complex of 1/1 stoichiometry between BPA and β-CD, with a high association constant, but no explanation was proposed concerning the origin of this high value as compared to results on other aromatic compounds with β-CD. In a study of cyclodextrin complexation by pairs with or without a phenolic hydroxyl group,[22] it was reported that additional hydrogen bond formation does not necessarily lead to enhanced stability of the complexes, due to the compensation between the enthalpic and entropic terms.[23] Consequently, the origin of the stability of BPA phenol derivative is still under discussion. In this work, we aim to investigate by spectrofluorimetry and ^{1}H NMR spectroscopy the formation, the stoichiometry, and the stability of inclusion complexes formed in aqueous solution between β-CD and four phenol derivatives: 4,4′-isopropylidenediphenol (BPA), 4,4′-(hexafluoroisopropylidene)diphenol (FBPA), IPP, and BIP. The stability of the complexes was studied with respect to two parameters (i) the molecular geometry, for which reason two bent molecules (BPA and FBPA) and two linear ones (IPP and BIP) were investigated, (ii) the presence of alkyl and phenol moieties; hence three molecules with alkyl side-chains were investigated: BPA, FBPA, and IPP.

The use of molecular modeling techniques for the study and investigation of the properties and 3D structures of such complexes has dramatically increased in recent years.[24,25] The combination of experimental and computational studies has been recognized as a powerful tool for the study of their geometries.[26] A molecular modeling study of complexation of benzoic acid and phenol with CDs using the AM1 method was reported by Ming-Ju Huang *et al*.[27] They show that the phenol hydroxyl group prefers to face the wider rim in the β-CD complex. We report here the results of semi-empirical molecular orbital calculations (in the gas phase and in the presence of solvent) performed by the AM1 method to investigate the formation of inclusion complexes between these phenol derivatives as guests and β-CD. Additionally, we analyze theoretical ^{1}H NMR chemical shifts for this phenol series at the Density Functional Theory (DFT) level.

RESULTS AND DISCUSSION

Spectrofluorimetry measurements

All phenols have strong absorption and emission bands in the UV-visible region; therefore, their interactions with β-CD can be studied without adding any chromophoric dyes.[28] The Benesi–Hildebrand method[29] was used to determine the stoichiometry and the association constants from fluorimetric measurements of the guest/β-CD systems. In all the systems, for $1/(I-I_0)$ *versus* $1/[\beta\text{-CD}]$, there are good linear correlations but not for $1/(I-I_0)$ *versus* $1/[\beta\text{-CD}]^2$. This indicates that only species of 1/1 stoichiometry are obtained, despite the high [guest]/[β-CD] ratios used.

In the case of the BPA/β-CD system, used by Del Olmo *et al*.,[21] the highest [BPA]/[β-CD] ratio was 0.83, whereas we started our experiments using a high concentration ratio: [BPA]/[β-CD] = 20 corresponding to a low β-CD concentration of $5\ 10^{-7}$ M. Even under these conditions, the fluorescence of BPA increases (Fig. 1), indicating a great affinity between BPA and β-CD. In this case, the binding constant at 25 °C is the same as that reported by Del Olmo *et al*.[21] This value is high for complexes based on non-covalent interactions.[30–32]

A great affinity is also observed in the FBPA/β-CD system. Indeed, at low concentration of $[\beta\text{-CD}] = 5 \times 10^{-7}$ M, there is a fluorescence increase (not shown). The binding constants K obtained by fluorimetric measurements at 25 and 35 °C for BPA/β-CD and FBPA/β-CD systems are given in Table 1 with the corresponding calculated thermodynamic data (ΔG°, ΔH°, and ΔS°). In the same Table 1 are listed the corresponding values for BIP/β-CD and IPP/β-CD obtained under the same experimental conditions. For these last two systems, the fluorescence emission of mixed solutions is practically constant up to a guest/β-CD ratio of 1, and increases for higher ratios.

$$\text{Guest} + \beta\text{-CD} \underset{k_{-1}}{\overset{k_1}{\rightleftharpoons}} \text{Guest}/\beta\text{-CD} \qquad (1)$$

The formation of inclusion complexes between the phenol derivatives and β-CD is favored in aqueous medium since the free energy variation is exergonic in all systems, as shown in Table 1. The stability constants of the two bent bisphenol (BPA and FBPA)/β-CD systems are higher than those for the complexes of linear guest (BIP, IPP)/β-CD systems. The stability constant K is the ratio between the threading rate constant k_1 and the

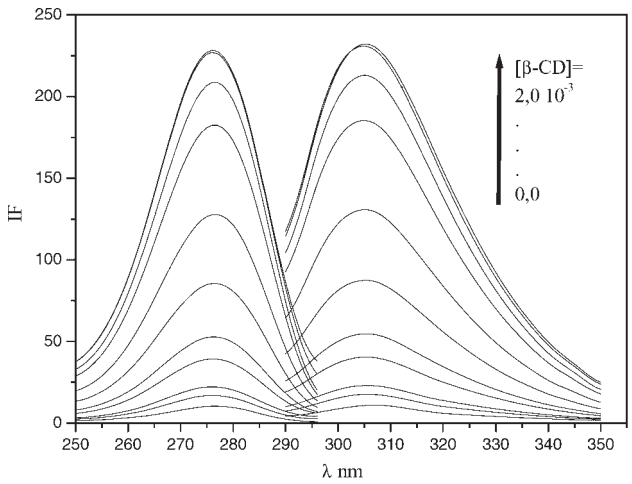

Figure 1. Excitation ($\lambda_{exc} = 276$ nm) and emission ($\lambda_{emis} = 305$ nm) curves of saturated aqueous BPA (10^{-5} M) solution at various β-CD concentrations (from 0 to $2\ 10^{-3}$ M)

DOI: 10.1002/poc

Table 1. Thermodynamic data for the equilibrium of β-CD with the various guests at 25 and 35 °C in aqueous medium

Guest	BPA		FBPA		BIP		IPP	
T°C	25	35	25	35	25	35	25	35
$10^{-3}K$ (M^{-1})	80 ± 12	61 ± 10	30 ± 8	8.0 ± 0.5	3.7 ± 0.6	2.9 ± 0.8	1.7 ± 0.7	1.3 ± 0.4
ΔG° (kJ mol^{-1})	-28.0 ± 0.4	-28.2 ± 0.4	-25.6 ± 0.7	-23.0 ± 0.2	-20.3 ± 0.4	-20.4 ± 0.7	-18.4 ± 1.2	-18.5 ± 0.9
ΔH° (kJ mol^{-1})	-20.7		-100.1		-19.8		-16.6	
ΔS° (J mol^{-1} K^{-1})	24.4		-250.5		2.2		6.0	

dethreading rate constant k_{-1} in equilibrium (1), $K = k_1/k_{-1}$. This ratio which indicates that the threading process is more rapid than the dethreading one in all the systems ($K > 1$), is greater for both bent molecules (BPA and FBPA) than for the linear ones (BIP and IPP). This can be explained by a more difficult dethreading process for bent molecules against threading one, whereas this is the less frequent case in linear molecules since this ratio is not as high as for bent molecules.

For three systems BPA/β-CD, BIP/β-CD, and IPP/β-CD, the reaction enthalpies show comparable values (ΔH° varies from -17 to -21 kJ mol^{-1}). The more exothermic values (more negative by about 4 kJ mol^{-1}) for BPA and BIP may be explained by the existence of two hydrogen-binding sites in BPA and BIP as compared to the IPP molecule, in which only one hydroxyl group is available.[22] Moreover, the entropic contribution originates from breaking of the solvent shell (a favorable entropy term) and from the binding process (unfavorable entropy term).[33] In these three systems (BPA/β-CD, BIP/β-CD, and IPP/β-CD), the entropic compensation is slightly favorable, and indicates that a gain in disrupting the solvent shell is sufficient to offset the entropy loss resulting from binding.

However, the FBPA/β-CD system shows markedly different behavior in the ΔS° and ΔH° values. Indeed, the entropic contribution in the FBPA/β-CD system is very negative, indicating that the entropy loss is large. The hydrophobicity of the FBPA molecule, which is greater than that of the three other phenol derivatives,[34,35] markedly disrupts the solvent sphere around free FBPA, whereas the formation of the complex leads to a better organization of the solvent shell. Concomitantly, a more exothermic enthalpy term (about four times higher than that of the other three systems) is obtained, arising from the stronger hydrophobic interaction resulting from the threading of the hydrophobic FBPA inside the β-CD cavity.[36]

^{1}H NMR measurements on phenol derivatives

In order to assign unambiguously the ^{1}H NMR signals and to detect the interaction site of the aromatic ring in the phenol derivatives, chemical shifts were calculated for each of the aromatic protons. The calculated ^{1}H NMR chemical shifts (δ_H^1) for the various phenols are listed in Table 2. The experimental values are obtained in solution, whereas the molecule is assumed to be isolated in the calculations. Nevertheless, the shifts of the H^a, H^b, and CH_3 protons are in the range of the appropriate experimental values. Note that the shifts of the ortho and meta protons of the phenyl groups were averaged out, assuming rapid rotation around the C—O axis in each case. Clearly, the results indicate that the most upfield hydrogens are the H^a atoms and the most downfield ones are the H^b atoms.

Except for FBPA, some tendencies appear clearly in the other systems: the ^{1}H NMR signals of the aromatic protons of free guests (H^a and H^b in Scheme 1) in D_2O appear as two sharp doublets (not shown). When the β-CD concentration increases, the H^a and H^b signals are slightly shifted upfield (Table 2) and become broader especially in the case of BPA and IPP, indicating formation of inclusion complexes in fast exchange with free β-CD. In contrast, in the FBPA/β-CD system, no

Table 2. Experimental and calculated ^{1}H NMR chemical shifts δ_H (ppm) of the aromatic part of the free phenol derivatives and in the presence of β-CD in D_2O

	BPA			FBPA		BIP		IPP		
	H^a	H^b	CH_3	H^a	H^b	H^a	H^b	H^a	H^b	CH_3
Free guest										
δ_H exptl	6.82	7.20	1.61	6.90	7.33	6.98	7.53	6.85	7.22	1.18
δ_H calc	5.93	6.62		5.75	6.54	6.05	6.75	5.96	6.58	
δ_H guest/β-CD	6.77	7.16	1.70	6.89	7.33	6.97	7.41	6.79	7.12	1.24

DOI: 10.1002/poc

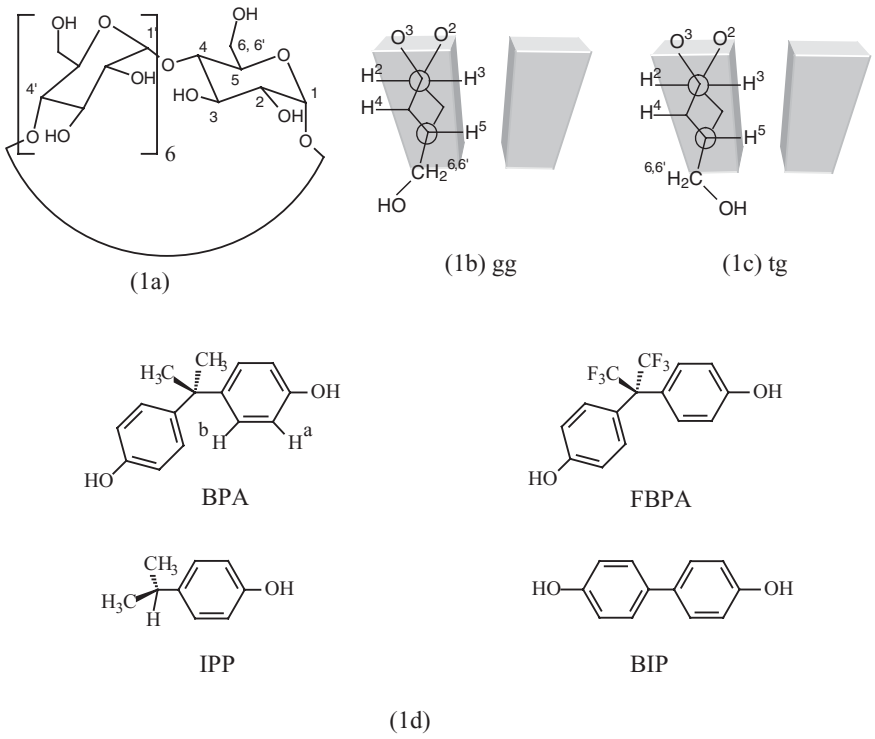

Scheme 1. Structures and numbering of: (**1a**) a glucopyranose unit in β-cyclodextrin, (**1b**) gg β-CD conformation; (**1c**) tg β-CD conformation; (**1d**) guest phenols

aromatic proton signal is changed (Table 2), indicating that they do not interact with β-CD. For the two guests IPP and BPA, the CH_3 protons are shifted downfield, indicating the involvement of the CH_3 moieties inside the β-CD cavity (Table 2).

^{1}H NMR measurements on cyclodextrin

The ^{1}H NMR signals of β-CD without guest and in the presence of the different phenol derivatives are presented in Fig. 2 on the same scale, in order to display the influence of the guest on the cyclodextrin protons. Generally, there are three groups of protons which are involved in host–guest inclusion compounds based on β-CD.[37]

The H^3 and H^5 protons located in the cavity of β-CD (Scheme 1) are shifted upfield in all the systems. This was taken as evidence for complex formation,[38] giving strong indications of the insertion of these guests into the β-CD cavity (Scheme 2). However, the H^3 proton in the case of the FBPA/β-CD system is more shifted than that in the other three systems. Probably, this proton is influenced by aromatic and non-aromatic groups; this indicates that the interaction of the first three guests (BIP, BPA, and IPP) involves the inner cavity more than does FBPA, and that FBPA interacts with β-CD from its wider rim. Moreover, the two $H^{6,6'}$ protons located in the narrower rim of the β-CD molecule are generally shifted when inclusion concerns this rim or when the guest is deeply inserted into the cavity. In our case, these two protons are affected in BIP/β-CD, BPA/β-CD, and IPP/β-CD systems, but are unchanged in the FBPA/β-CD complex. This again indicates that the inclusion of all the guests is deep and involves the narrower rim, except for FBPA, where it seems that inclusion is not deep and that the interaction occurs far from these protons. The H^2 and H^4 protons, which are located outside the cyclodextrin cavity, are only shifted in the BPA/β-CD and FBPA/β-CD systems, especially in the latter. This seems to indicate that the interaction between FBPA and β-CD occurs more outside the cavity than inside it (cf. H^2 and H^4 proton signals), and appears to be quite different from that of the other three guests (Scheme 2).

In addition, 1D-ROESY experiments were performed to obtain more detailed information on the molecular geometry of these complexes.[39] Aromatic protons or methyl groups were selectively excited and the response of the various β-CD protons observed. Table 3 lists the ROE enhancements, and Fig. 3 depicts the 1D-ROESY spectrum of BPA.

For the IPP/β-CD complex, selective excitation of H^a and H^b produced ROE signals for all the protons inside the cavity; no ROE was observed for H^2 and H^4. This indicated that IPP is completely included in the cavity. The relatively large ROE values observed for H^3, after

DOI: 10.1002/poc

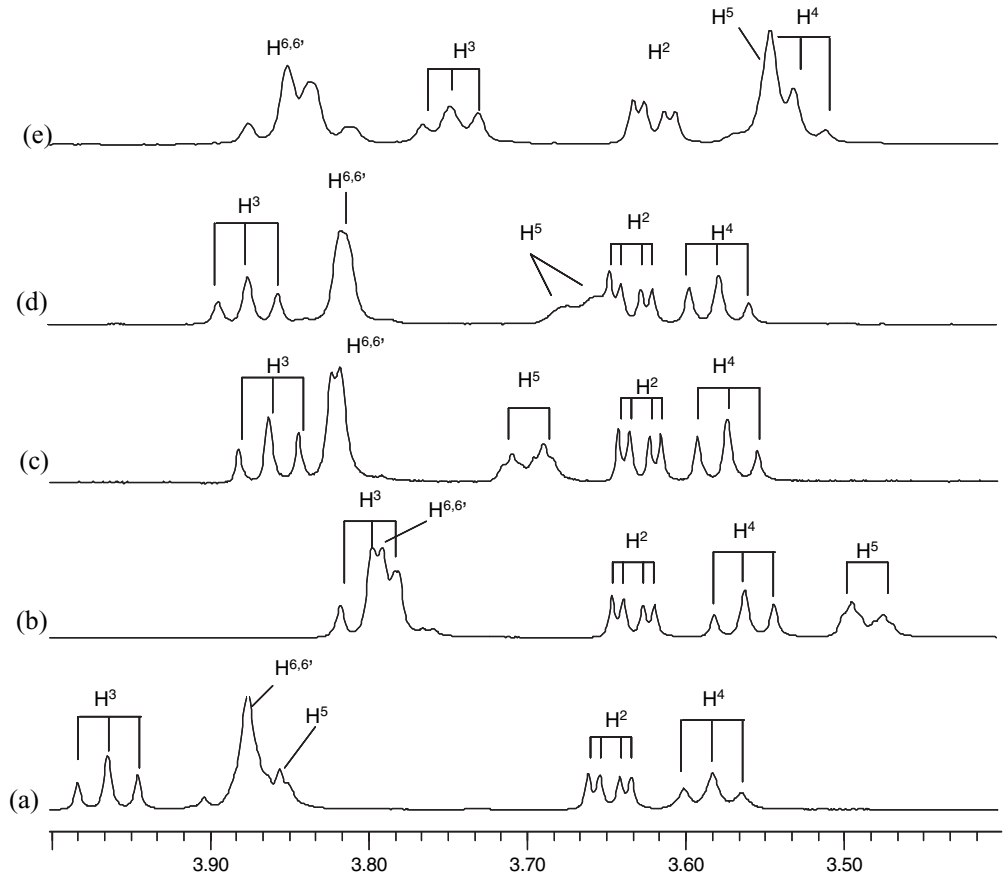

Figure 2. ^{1}H NMR (500 MHz) spectra in D_2O of β-CD free (a) and in presence of BPA (b), BIP (c), IPP (d), FBPA (e)

selective excitation of CH_3, indicate that the phenol moiety of IPP is near the narrower rim and that the methyl groups are near the wider one (Table 3).

In the case of the BPA/β-CD complex, the ROE response was very similar for the aromatic proton pairs H^a, H^b with H^5, H^3 (5.2; 5.9% for H^a and 5.3; 4.1% for H^b); the ROE value for $H^{6,6'}$ and H^a shows that BPA is deeply inserted. The selective excitation of CH_3 gave enhancement exclusively on H^3. No ROE signal was observed between $H^{6,6'}$ and CH_3 (Table 3, Fig. 3). These results show that complexation occurs through the inclusion of the phenyl moiety in the hydrophobic cavity of β-CD and that the molecule enters the cavity very deeply and from the wider rim.

For the BIP/β-CD complex, selective excitation of H^a and H^b produced ROE signals for all the protons inside the cavity and also with $H^{6,6'}$; no ROE was observed for H^2 and H^4. This result shows that BIP is deeply included in the cavity (Table 3).

For the FBPA system, selective excitation of H^a and H^b produced ROE for H^3, H^2, and H^4. The larger ROE values observed for H^4 indicate that H^a is located outside the cavity nearer to H^4 than to H^3. No ROE was observed for H^5 and $H^{6,6'}$. The average distance between H^a and the protons H^2 and H^4 should be larger than that between H^b and the same proton because their ROE values are about six times larger.

To investigate the nature and the location of the interaction between β-CD and FBPA, we studied the ^{19}F NMR signal of free FBPA and FBPA in the presence of increasing concentrations of β-CD (Fig. 4).

The spectra show that there are no separate resonances for the fluoromethylene group of FBPA in the free and included states for the two ratios,[40,41] and indicates that exchange between the environments is fast on the NMR time scale, according to Eqn (1).

Some broadening of the fluoromethylene group signal of FBPA is observed in the presence of β-CD. For a 1/1 ratio of FBPA/β-CD, the width at half-height is greater (42.4 Hz) than that of free FBPA (5 Hz). This signal represents the superposition of the spectrum of bonded and free FBPA species. However, for a 1/6 ratio, the width at half-height is 29.3 Hz, indicating that the equilibrium is displaced towards the complex, resulting in fewer free molecules.[11] Alderfer *et al.*[42] in the study of the inclusion of 4-fluorophenol in the cavity of α-CD in aqueous solution, reported that the hydrophilic OH of the phenol is outside the hydrophobic cyclodextrin cavity, while the fluorine atom is located inside, and that complexation is mainly driven by dispersive and hydrophobic inter-

DOI: 10.1002/poc

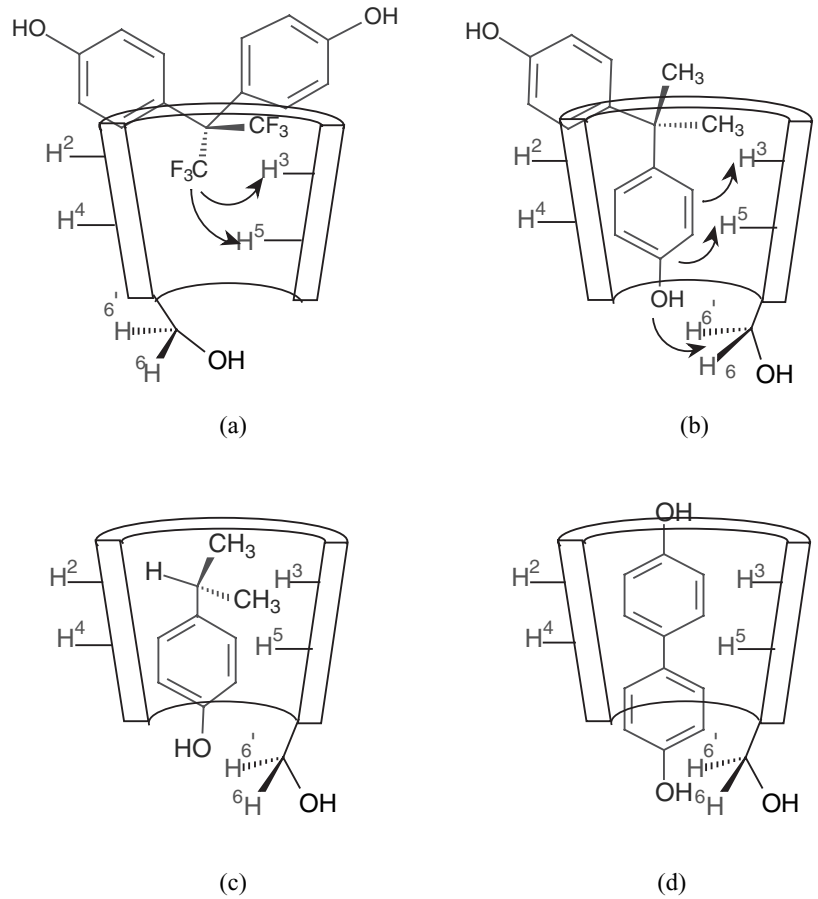

Scheme 2. Proposed structures for different inclusion complexes: (**a**) FBPA/β-CD ('tail-first'); (**b**) BPA/β-CD ('head-first'); (**c**) IPP/β-CD, (**d**) BIP/β-CD

actions. In our case, the chemical shift of the fluoromethylene group of FBPA goes downfield when β-CD is added. This suggests that the inclusion of this group in the cavity is favored by hydrophobic interactions between fluoromethylene and β-CD (Scheme 2).

Molecular orbital modeling studies of the guest/β-CD complexes

Since the β-CD structure exhibits some flexibility[43] and among the various possible geometries, two different conformations of β-CD (labeled as gg, tg) were chosen to model the complex (Scheme 1). Our primary purpose is to explore how complexation properties can be modulated by the host conformation. The values of the interglucopyranose bonds and torsion angles involving the C(4)—O(4)—C(1′) reflect the macrocyclic conformations. The gg and tg conformations show a regular conformation of the glucopyranosyl rings, that is, with C_7 symmetry. The gg and tg conformations differ mainly in the O(6)—C(6)—C(5)—O(5) dihedral angle which reflects the conformation of the C(5)—C(6) bond in glycopyranose residues. In the gg conformation, this dihedral angle is -81° with the O—H bond oriented parallel to the glucopyranose ring and directed toward the

Table 3. ROE enhancements (%) obtained on selective excitation of aromatic protons or methyl groups of different complexes

	BPA			FBPA		IPP			BIP	
	H^a	H^b	CH_3	H^a	H^b	H^a	H^b	CH_3	H^a	H^b
H^3	5.2	5.3	11.5	4.7	2.9	1.3	1.5	2.7	1.1	1.6
H^5	5.9	4.1	2.9	—	—	2.3	2.5	0.8	1.5	2.3
$H^{6,6'}$	0.5	—	—	—	—	0.8	0.6	0.2	0.6	0.8
H^2	—	—	1.1	3.5	0.4	—	—	—	—	—
H^4	—	—	1.2	6.8	1.1	—	—	—	—	—

DOI: 10.1002/poc

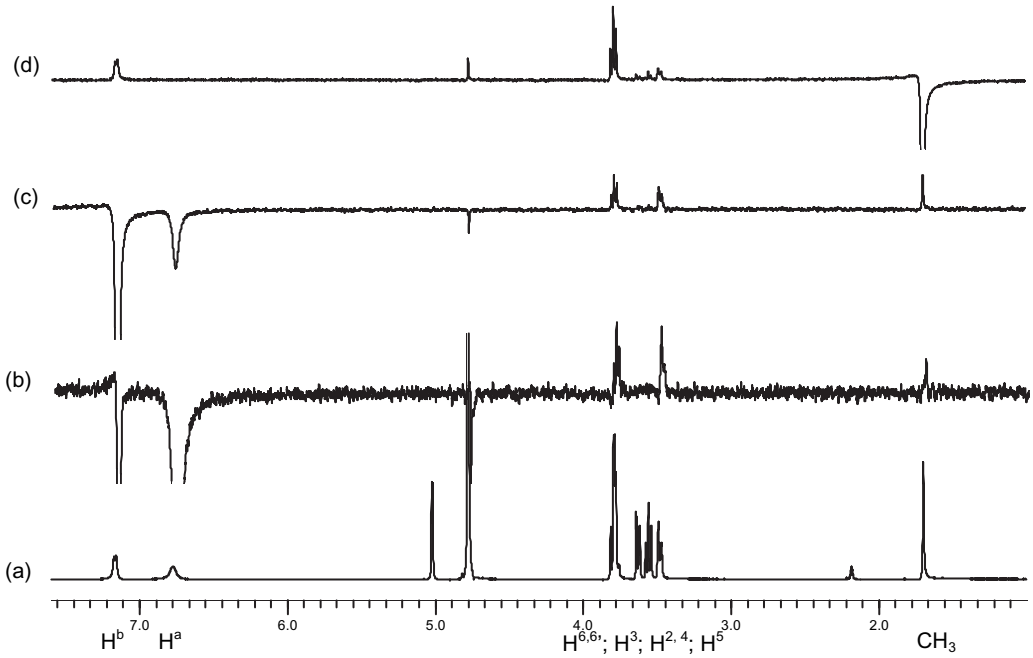

Figure 3. NMR (500 MHz) spectra for 1D-ROESY experiments on the BPA/β-CD complex: (a) base spectrum; (b) selective excitation of H^a; (c) selective excitation of H^b; (d) selective excitation of CH_3

O(5) of the adjacent glucose residue (Scheme 1). The O(5′)...H—O(6) and O(5′)...O(6) distances are 2.21 and 3.10 Å, respectively, suitable for hydrogen bond formation. In the tg conformation, the O(6)—C(6)—C(5)—O(5) angle is 106° and the O(6)—C(6) bond is directed towards the inside of the cavity. In this conformation, the O(6)—H bond is directed toward the O(6′) of the adjacent glucopyranose residue. The O(6′)...H—O(6) and O(6)...O(6′) distances are 2.16 and 3.10 Å, respectively. Another type of hydrogen bond occurs in this conformation and involves the H(6) and O(6′) atoms (H(6)...O(6′) = 2.23 Å). Calculations indicate that the gg conformation, which is found to be the more stable in solution, is not the most stable in the gas phase, whereas the tg conformation is more favorable in the gas phase. However, the solvent effect strongly

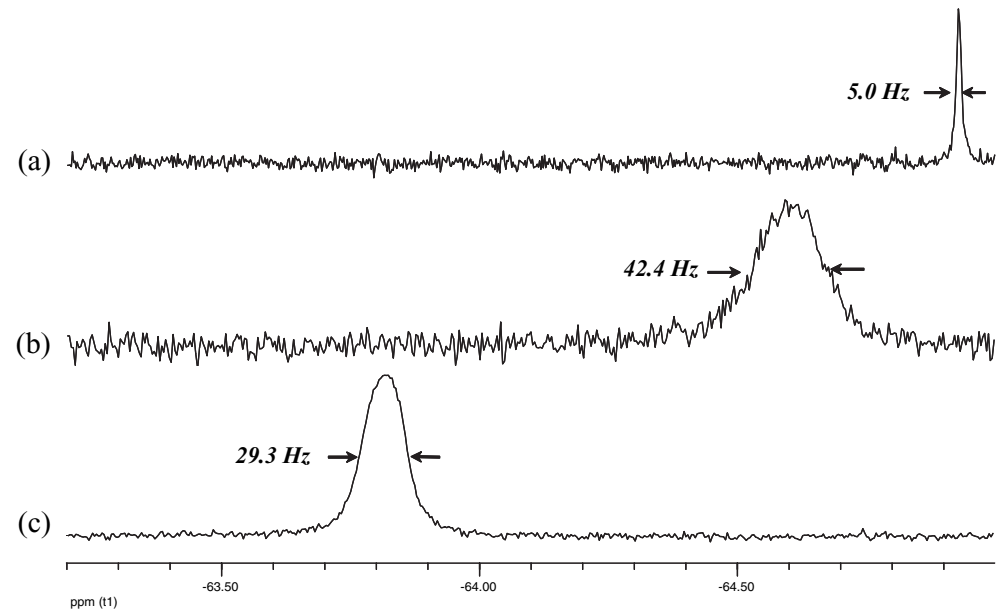

Figure 4. Effect of β-CD on the ^{19}F NMR (282.35 MHz) spectra of FBPA in D_2O at 25 °C: (a) without β-CD, (b) FBPA/β-CD: 1/1, and (c) FBPA/β-CD: 1/6

DOI: 10.1002/poc

stabilizes the gg conformation of β-CD, since many hydrogen-bonding interactions with the solvent can occur with the primary OH groups oriented towards the exterior of the cavity. To estimate the solvent effect on the relative energies of both conformer, we performed, therefore, the enthalpies of solvation are -385 and -310 kJ mol^{-1} for the gg and the tg conformers, respectively (MPWB1K/6-31G(d) single-point calculations using the COSMO solvation model).

The initial geometries of guest/β-CD complexes are constructed by bringing the guest up to the cavity. For the BPA/β-CD and FBPA/β-CD complexes, a preliminary study was undertaken on the host to ensure that the most stable conformation was taken to construct the complex. Among all possible conformations (defined by the torsion angles ϕ_1 and ϕ_2 between the plane defined by the C—C(CH$_3$)$_2$—C angle and those of the aromatic rings; see some particular conformations in Scheme 3), the C_2 conformation was found to be the most stable at the AM1 and B3LYP/6-31G(d) levels of calculation.

Two orientations of the guest were considered. In the first orientation, named 'head-first,' an aromatic ring is introduced into the cavity leaving the alkyl groups outside. The second orientation, 'tail-first,' involves the inclusion of the methyl groups in the cavity leaving the phenol groups more or less outside (Scheme 2). The energy change associated with complexation can be expressed using the following Eqn (2). The interaction energy (ΔE_{11}) is defined as the difference between the energy of the complex (when the guest is inside the cavity) and the sum of the energies of the isolated host and guest.

$$\Delta E_{11} = E_{\text{complex}} - E_{\text{guest}} - E_{\beta\text{-CD}} \qquad (2)$$

where E_{complex}, E_{guest}, and $E_{\beta\text{-CD}}$ are the total energies of the 1/1 complex, of the free guest, and of the free host (β-CD), respectively. It should be kept in mind that the calculated values of interaction energies cannot be directly compared with the experimental data obtained in aqueous solution. Our calculations are performed on molecules in the gas phase, without thermal correction of the energy and entropy. However, the calculations can reflect the stabilization forces established in the cavity after inclusion, which contribute to the total formation enthalpy, ΔH_f°, of the complex. Although the formation enthalpies can be easily calculated by semi-empirical methods, such thermodynamic parameters are not directly accessible by *ab initio* or DFT calculations. The thermodynamic data require much more effort at the Hartree–Fock or DFT levels. Therefore, we use the interaction energies to quantify the interaction between guest and host in the optimized geometries.

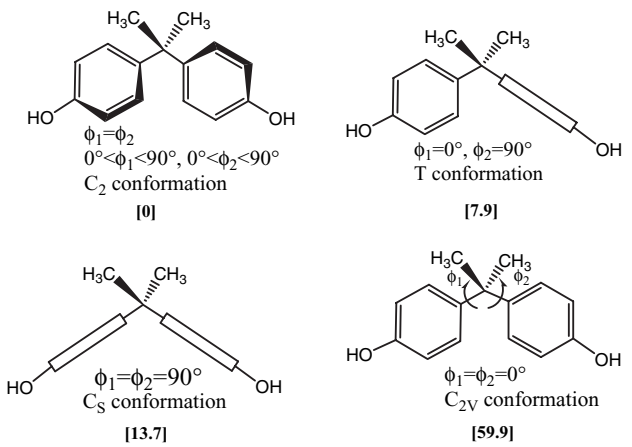

Scheme 3. Possible conformations with different symmetries of BPA. Relative energies (in kJ mol^{-1} and calculated at the B3LYP/6-31G(d) level of calculation) of the conformer are given in brackets

Interaction energies

Table 4 contains the interaction energies, ΔE_{11}, of the inclusion complexes of BPA, FBPA, BIP, and IPP with β-CD in the 'head-first' and 'tail-first' orientations of the guest (Scheme 2). Two sets of interaction energies, ΔE_{11}, are reported in Table 4 corresponding to the gg and tg conformations (Scheme 1).

AM1 calculation. In Table 4, AM1 results reveal that the energies of the complexes are consistently lower than the sum of the energies of the corresponding isolated host and guest, and the interaction energies range from -8.2 to -24.5 kJ mol^{-1}. However, the interaction between host and guest in the complex strongly depends on the conformation of the host. When β-CD is in the gg conformation, a marked preference for the inclusion of the guest in the 'tail-first' orientation is found, and in vacuum, the interaction energies are in the order FBPA $\approx$ BPA $<$ IPP. The tg conformation shows an opposite preference for the guest orientation, since the calculations suggest that the more stable structure is obtained when the phenol group is included in the hydrophobic cavity ('head-first') and the interaction energies are found in the order FBPA $<$ BIP $\approx$ BPA $<$ IPP. Beyond the preference for the 'head-first' orientation, the tg conformation allows to obtain complexes having a stronger interaction, and the interaction energies with the tg conformation are more than 5 kJ mol^{-1} lower than with gg. Probably the deeper penetration of the guest into the cavity (see optimized geometries in the next section) in the tg conformation makes it possible to establish a larger number of van der Waals interactions. Whatever the orientation of the host with respect to the cavity, the results indicate that bent guests interact more strongly than linear ones when β-CD is in the gg conformation, that is, the most stable conformation in solution, and the overall order of interaction energies is FBPA $\approx$ BPA $<$ BIP $<$ IPP which is in good agreement with the experimental findings.

DOI: 10.1002/poc

Table 4. Interaction energies (ΔE_{11} in kJ mol^{-1}) of the 1/1 complexes in two orientations

	BPA		FBPA		BIP	IPP	
	Head-first	Tail-first	Head-first	Tail-first	Head-first	Head-first	Tail-first
Gas phase							
AM1							
$\Delta E_{11(gg)}$	−11.4	−20.3	−9.5	−20.4	−8.2	−12.1	−13.1
$\Delta E_{11(tg)}$	−21.4	−19.0	−24.5	−16.2	−22.9	−17.9	−16.0
MPWB1K//AM1							
$\Delta E_{11(gg)}$	−41.4	−45.8	−34.9	−57.0	−28.2	−28.9	7.5
$\Delta E_{11(tg)}$	−46.2	−57.6	−41.1	−68.5	−36.7	−34.2	−42.5
Water							
MPWB1K//AM1							
$\Delta E_{11(gg)}$	−13.3	−23.6	−6.6	−29.5	6.5	−3.8	12.4
$\Delta E_{11(tg)}$	−13.1	−34.4	−10.5	−38.0	−13.7	−8.8	−25.8

DFT calculation. The interaction energies calculated with the meta hybrid functional MPWB1K are significantly more negative than the AM1 values. As the functional MPWB1K allows a better description of the non-bonded interactions and especially weak interactions, this result strongly suggests that the complexation process is driven by weak interactions such as dispersive forces.[44] Considering the most stable gg conformation in solution for better comparison with experimental results, DFT calculations indicate an order of interaction energies (FBPA < BPA < BIP ≈ IPP) which is in agreement with experimental results. Interestingly, addition of a phenolic substituent to IPP leads to the highest interaction energies with β-CD. This result indicates that the phenolic group of BPA which is not included in the cavity nevertheless plays a specific stabilizing role in the complexation process.

The FBPA/β-CD system is somewhat surprising in that the interaction energy increases markedly when electron correlation (through MPWB1K/6-31G(d) calculations) is taken into account ($\Delta E_{11} = -57.0$ and -68.5 kJ mol^{-1} for the complex with β-CD in the gg and tg conformation, respectively). Furthermore, the interaction energy resulting from the 'tail-first' orientation is considerably smaller than for the 'head-first' orientation. This result strongly suggests that the mode of inclusion is somewhat different from that of the other guests and that the inclusion of FBPA most probably involves the threading of the alkyl group rather than the OH group, as concluded from the NMR experiments.

Solvent effects. In order to check the role of the solvent, which is known to have very large effects on complex formation and energy variation, we represented the solvent by the continuum model (COSMO model). The resulting interaction energies increase markedly and become positive in some cases. The results confirm, however, the order of interaction energies found in the gas phase. However, the results in solution can be considered as indicative and show some tendencies, even if solvent reorganization involved in the solvation process is not considered in the model: bent molecules interact more strongly with β-CD than linear ones, while for FBPA/β-CD system, the 'tail-first' is the more stable orientation. Furthermore, the failure of the continuum solvation model in the study of supramolecular systems has been mentioned recently,[45] suggesting that an explicit solvation model should be used in combination with the continuum model to obtain quantitative results.

Optimized geometries of the complexes

The optimized geometries of the complexes are displayed in Fig. 5 for BPA/β-CD, FBPA/β-CD, and IPP/β-CD and in Fig. 6 for BIP/β-CD. The depth of inclusion of the guest in the host cavity can be defined as the distance separating the barycenter of the cyclodextrin (this point almost coincides with the barycenter of the seven glycosidic oxygen atoms) and the para carbon of the phenol group located inside the cavity. The measured distances in the 14 possible complex structures are presented in Table 5 (taking into account the gg and tg conformations of β-CD, as well as the 'head-first' and 'tail-first' inclusions of the guest in the cavity). The geometry of the complex depends on the nature of the guest and, if we consider first the 'head-first' orientation, the depth of inclusion ranges from 1.55 to 2.88 Å. This indicates partial inclusion of the phenolic group in the cavity (the half height of β-CD is about 3 Å). Except for IPP, the guest is found to be inserted more deeply into the cavity when β-CD adopts the tg rather than the gg conformation. This result can be explained by the change in the shape of β-CD when the intramolecular hydrogen bonds between primary hydroxyl groups are established. Indeed, in this conformation the cone shape is more pronounced and the diameter of the wider rim increases, which allows deeper penetration. In this respect, the effect of the β-CD

DOI: 10.1002/poc

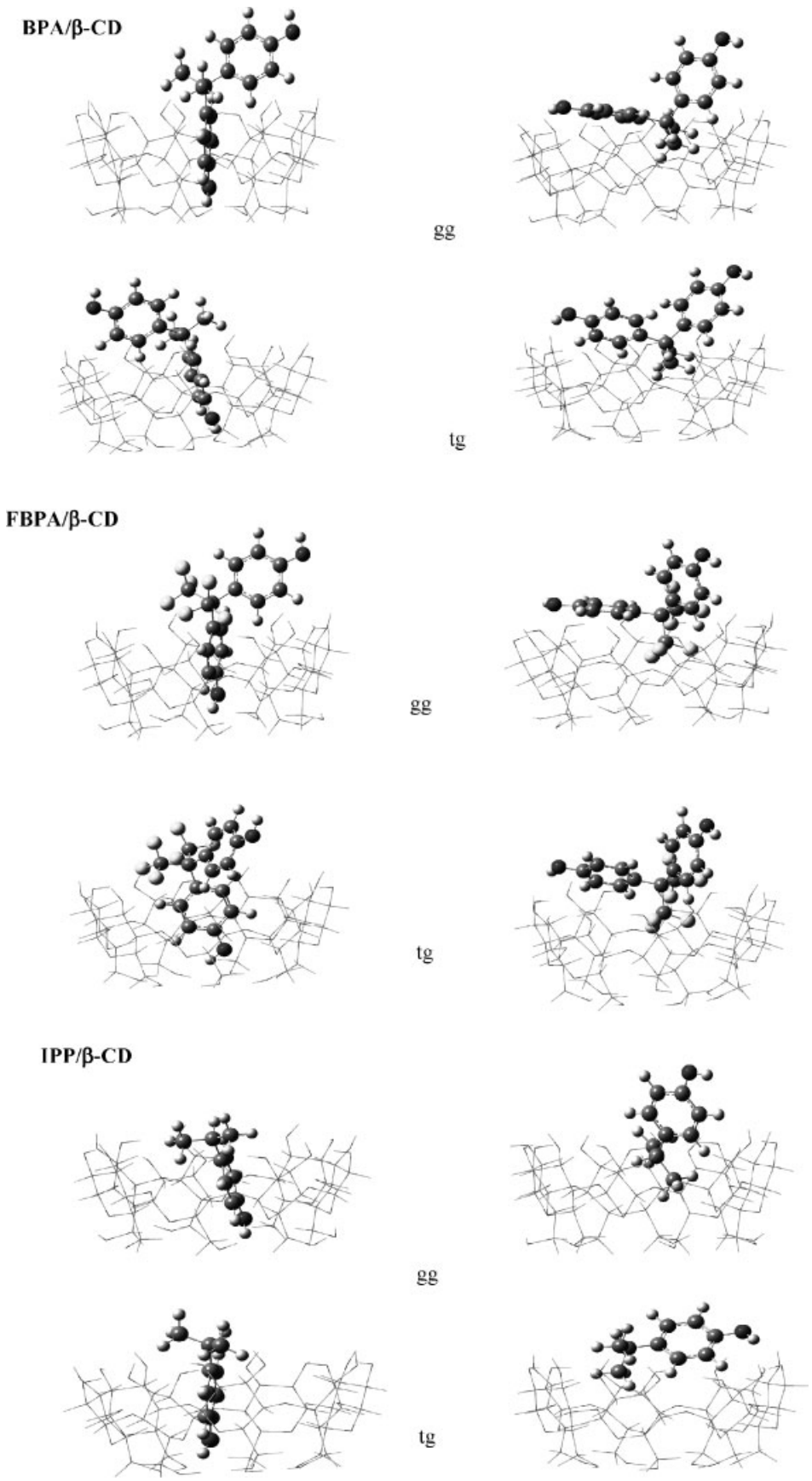

Figure 5. Optimized structure of guest/β-CD inclusion complexes (AM1 calculations). For the complexes involving BPA, FBPA, and IPP compounds, the 'head-first' and 'tail-first' complexes are displayed on the left and right, respectively

DOI: 10.1002/poc

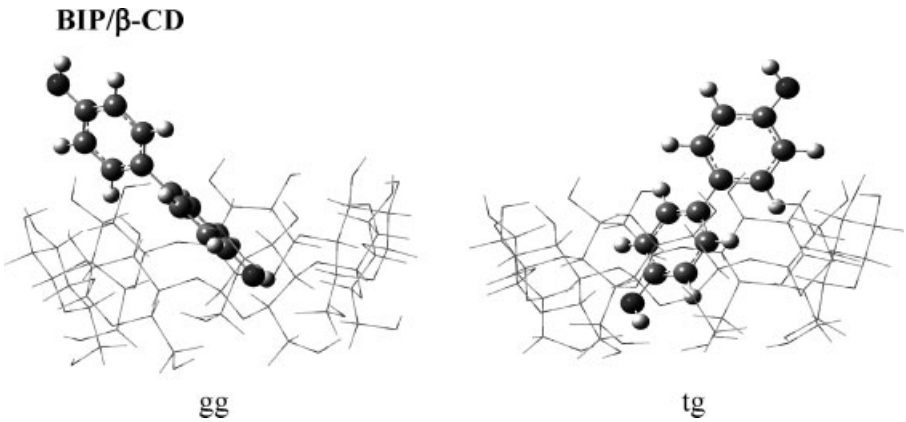

Figure 6. Optimized structure of BIP/β-CD inclusion complexes (AM1 calculations)

conformation is particularly spectacular when BIP is included in the cavity, since the distance of inclusion decreases from 2.88 to 1.81 Å. It should be also noted that the direction of approach of BIP strongly deviates from the vertical symmetry (C_7) axis of the β-CD, which suggests attractive interactions between the aromatic rings of BIP and both the hydrophobic cavity and the wider rim of β-CD. For BPA, FBPA, and IPP in the 'head-first' orientation, the phenolic group is almost aligned with the vertical axis of β-CD, and close contact with cyclodextrin involves the methyl or CF_3 groups.

CONCLUSIONS

From a general point of view, the present experimental and theoretical investigation provides a comprehensive picture of the interactions of some phenolic derivatives with β-CD, highlighting the following aspects: (i) the binding mode and stoichiometry of the inclusion complexes of phenolic derivatives with β-CD, (ii) the interactions involved in the complexation process, (iii) the influence of the β-CD conformation and the guest structure on the binding energy.

More precisely and in agreement with the results of Del Olmo *et al*. on the BPA/β-CD system, our study on the interaction between β-CD and phenol derivatives show that complexes with BPA, and with fluorinated FBPA are more stable than those with IPP and BIP. This difference between the bent and linear molecules originates from the difference in geometries which, in the case of bent molecules, seems to enhance its interaction of the guest with β-CD and to prevent its unthreading. Moreover, in the optimized geometry of the BIP/β-CD complex, a particular strong deviation of the principal axis of BIP from the vertical symmetry axis (C_7) of β-CD occurs (Fig. 6). For bent molecules, the same sort of deviation is due to the second aromatic residue, which is located outside the cavity, approaching the wider rim of β-CD (Fig. 5), probably because of the van der Waals interactions. The stability of the complexes of β-CD with linear molecules is comparable to that with other linear aromatic compounds such as biphenyl, bithiophene, nitrophenol . . . Moreover, in the FBPA/β-CD system, both experimental results and theoretical calculation show a different complexation mode from that of the other three systems. Indeed, the 'tail-first' complexation mode is the most probable one, where complexation occurs through the wider rim of the cavity, the fluorinated alkyl groups interacting with the β-CD inner cavity. This complexation mode is deduced from experimental measurements (NMR) and is also predicted by DFT calculations. DFT calculations indicate high interaction energy comparable to the formation enthalpy deduced from experimental results on the FBPA/β-CD system. This agreement indicates that DFT calculations

Table 5. Calculated distances *d* between the para carbon of the phenol group and the barycenter of the seven glycosidic oxygens of β-CD

	BPA	FBPA	BIP	IPP
gg				
Head-first	2.11	2.33	2.88	1.55
Tail-first	2.58	3.20		2.76
tg				
Head-first	2.10	2.22	1.81	2.10
Tail-first	2.95	3.56		3.61

DOI: 10.1002/poc

(MPWB1K//AM1) are a useful predictive tool for such series. It has been reported as suitable for describing weak non-covalent interactions for simple systems,[46] and also seems to be useful for systems as large as ours.

EXPERIMENTAL

Chemicals

BPA and FBPA (Acros) were purified by double recrystallization from toluene (Merck); IPP (Aldrich) was purified by sublimation at 50 °C; BIP (Acros) was purified by recrystallization from ethanol; β-cyclodextrin (Sigma) was used as received. Distilled water was purified by a Millipore system and was used for aqueous solutions.

Spectrofluorimetric measurements

Fluorescence spectra were obtained with an Aminco–Bowman series 2 luminescence spectrometer equipped with a thermostated cell-carrier. An initial 10^{-2} M solution of guest (g) in ethanol was prepared. From this solution, we prepared a 10^{-5} M solution of guest in H_2O. Different concentrations of β-CD were prepared (4×10^{-2} M, 10^{-3} M, 10^{-4} M). For 10 mL of the aqueous guest solution, small amounts of the aqueous solution of β-CD were added to obtain different [guest]/[β-CD] ratios with a constant concentration of the guest at about 10^{-5} M. The maximum volume added did not exceed 400 μL. Fluorescence measurements were performed on 3 mL samples at two temperatures, 25 and 35 °C.

NMR measurements

^{1}H NMR spectra at 25 °C were recorded on a Bruker DRX500 spectrometer at 500 MHz with a TXI probe. Saturated solution (1.5 mL) of guest in D_2O was prepared. To this solution, small amounts of β-CD were added successively at different [guest]/[β-CD] ratios. Chemical shifts (δ) are given in ppm with respect to solvent ($\delta_{HDO} = 4.78$). ^{19}F NMR spectra were run on a Bruker CXP NMR spectrometer at 282.35 MHz locked on the D_2O deuterium frequency. 1D ROESY experiments used the standard Bruker 'selrogp' pulse program, with a 300 ms spinlock pulse for mixing, and a recycling time of 4.57 s.

Computational details

The molecular orbital study was performed on each isolated phenol derivative and on its 1/1 inclusion complexes with β-CD.

Calculations on guests. Calculations were performed using the AM1[47] method implemented in the AMPAC package.[48] The minimum of the potential energy surface as well as characteristic points on this surface were further optimized using the more refined DFT method with the B3LYP functional[49] and 6-31G(d) basis set.[50] The DFT results reported here were obtained using Gaussian 98.[51] Isotropic NMR chemical shielding was also evaluated for each compound by means of the GIAO (Gauge-Independent Atomic Orbital) method[52] as implemented in Gaussian 98. Chemical shifts δ_i were calculated by subtracting the appropriate isotropic part σ_i of the shielding tensor from that of a standard compound σ_{st}, that is, $\delta_i = \sigma_{st} - \sigma_i$ (ppm). The isotropic shielding constant calculated for TMS using the same method and the same basis set was 32.18 ppm for the ^{1}H nucleus.

1/1 Complexes of phenol derivatives with β-CD. The β-CD complexes consist of 180 atoms, which makes the use of sophisticated methods such as *ab initio* calculations, computationally time-expensive and impractical for exploring the potential energy surface for such large systems. Therefore, we used the semi-empirical AM1 method to optimize the geometries of the inclusion complexes. This method was chosen because it has been proven that it is able to reproduce satisfactorily the experimental geometry for such molecules.[53] Furthermore, it has been shown that AM1 calculations are better able to treat long-range dispersion interactions, generally denoted as van der Waals interactions, than PM3[54] calculations. While no specific parameters are included in semi-empirical energy functions to express the dispersion term, previous studies indicate that AM1 produces qualitative results to describe this effect.[55] The geometry of β-CD was fully optimized without imposing any symmetry restrictions and this was followed by harmonic frequency analysis to ensure that the stationary point located was the true minimum (all eigenvalues of the Hessian matrix were positive). The starting geometry for β-CD used before optimization was based on its crystallographic structure as determined by X-ray diffraction data in the Cambridge data bank.[56] All geometry optimizations were carried out considering molecules in the gaseous state. The inclusion complex was constructed from separately AM1-optimized β-CD and the corresponding guest geometries. A preliminary calculation was undertaken to determine the orientation of guest inclusion. It is found that the approach of the OH group of the phenol through the wider rim of β-CD is more favorable in energy than through the narrower, with an energy difference of 3.3 kJ mol^{-1}. On the basis of this result, it was assumed that in all the guest/β-CD systems, complexation occurs only through the wider rim of the cavity.

Finally, DFT single-point calculations using the 6-31G(d) basis set were performed on the AM1-optimized geometries of complexes, both *in vacuo* and

DOI: 10.1002/poc

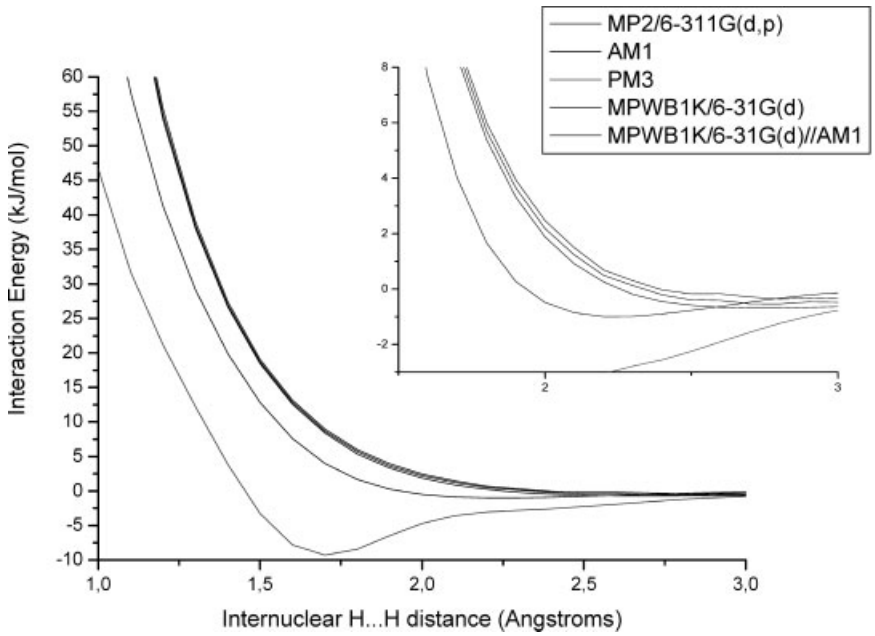

Figure 7. Energy profiles as a function of H . . . H intermolecular distance between two methane molecules arranged in a staggered orientation. Ordering of the profiles at 2 Å from top to bottom: MPWB1K/6-31G(d)//AM1, MPWB1K/6-31G(d), MP2/6311G(d,p), AM1, and PM3

in water solution by using the COSMO[57] continuum solvation model based on the self-consistent reaction field. Although current density functionals can describe hydrogen bonds with good accuracy,[58] they fail to do so for the description of van der Waals interactions.[59] In recent years, new density functionals have been developed that allow the correct treatment of the non-bonded interactions such as van der Waals interactions. Therefore, we used the MPWB1K[60] hybrid meta GGA functional since it was recommended recently as the best of 44 DFT methods tested. Among 44 tested DFT methods, MPWB1K was found to give the best performance for weak interactions. More generally, it has been shown from experiment that short-range H . . . H intermolecular interactions between guest and host are important in controlling the geometry of the complex. Therefore, we determine the CH_4 dimer interaction potential energy surface with different methods to evaluate the performance of our methodology, that is, the combination of AM1 semi-empirical method for geometries optimization with MPWB1K for single point calculation.

The interaction of methane dimer in staggered orientation as a function of H . . . H distance is displayed in Fig. 7. The energy profile calculated at the MP2/6-311G(d,p) level of calculation is taken as the reference. The MP2/6-311G(d,p), MPWB1K/6-31G(d), and MPWB1K/6-31G(d)//AM1 show similar smooth repulsion profile with a minimum located at 2.8 Å and an interaction energy in the range of −0.68 to −0.5 kJ/mol. PM3 predict an unphysical minimum (at 1.7 Å with interaction energy of −9.30 kJ/mol), while an excellent agreement between MPWB1K/6-31G(d) and MP2/6-6311G(d,p) is obtained. The AM1 calculations shows weaker repulsion than MP2/6-311G(d,p) having a minimum at 2.2 Å and interaction energy of −0.99 kJ/mol. In conclusion, the combination of AM1 geometries with single point MPWB1K/6-31G(d) seems a valuable methodology to quantify the long-range H . . . H intermolecular interactions for large host–guest systems.

Acknowledgements

The authors acknowledge the French Embassy (Tunisia) and the Ministry of Foreign Affairs (France) for financial support to S. Chelli. Dr J. S. Lomas is also gratefully thanked for his kind help in revising the manuscript, Mrs E. Benzarti (Faculté des Sciences; Monastir; Tunisia) for the ^{19}F NMR analyses, and Dr B. Fenet (Centre Commun de RMN/EZUS, Lyon 1, France) for the 1D ROESY NMR experiments.

REFERENCES

1. Lehn JM. *Supramolecular Chemistry Concepts and Perspectives*. VCH: New York, 1995.
2. Sauvage JP. Dietrich-Buchecker C. *Molecular Catenanes, Rotaxanes and Knots: A Journey through the World of Molecular Topology.* Wiley-VCH: New York, 1999.
3. Fyfe MCT, Stoddart JF. *Acc. Chem. Res.* 1997; **30**: 393–401.
4. Whitesides GM, Simanek EE, Mathias JP, Seto CT, Mammen DN, Gordon DM. *Acc. Chem. Res.* 1995; **28**: 37–44.
5. Rao VP, Turro NJ, Ramamurthy V. *Tetrahedron Lett.* 1989; **30**: 4641–4644.

DOI: 10.1002/poc

6. Shen X, Belletete M, Durocher G. *Langmuir* 1997; **13**: 5830–5836.
7. (a) Lagrost C, Lacroix J-C, Aeiyach S, Jouini M, Chane-Ching KI, Lacaze PC. *J. Chem. Soc. Chem. Commun.* 1998; 489–490; (b) Bergamini JF, Belabbas M, Jouini M, Aeiyach S, Lacroix J-C, Chane-Ching KI, Lacaze PC. *J. Electroanal. Chem.* 2000; **482**: 156–167.
8. Rendenti E, Szente L, Szejtli J. *J. Pharm. Sci.* 2000; **89**: 1–8.
9. Nasongkla N, Wiedmann AF, Bruening A, Beman M, Ray D, Bornmann WG, Boothman A, Gao J. *Pharma. Res.* 2003; **20**: 1626–1633.
10. Breslow R, Dong SD. *Chem. Rev.* 1998; **98**: 1997–2011 and references therein.
11. Binkowski C, Cabou J, Bricout H, Hapiot F, Monflier E. *J. Mol. Catal. A: Chem.* 2004; **215**: 23–32.
12. Kitano H, Taira Y, Yamamoto H. *Anal. Chem.* 2000; **72**: 2976–2980 and references therein.
13. Schnell H. *The Chemistry and Physics of Polycarbonates*. Wiley: New York, 1964.
14. Cort AD, Nissinen M, Mancinetti D, Nicoletti E, Mandolini L, Rissanen K. *J. Phys. Org. Chem.* 2001; **14**: 425–431.
15. Ochi M, Morishita T, Kokuhu T, Harada M. *Polymer* 2001; **42**: 9687–9695.
16. (a) Vani JNR, Vijayalakshmi V, Chatterjee PC. *J. Adhes. Sci. Technol.* 1991; **5**: 1001–1011; (b) Vani JNR, Vijayalakshmi V, Chatterjee PC. *J. Adhes. Sci. Technol.* 1992; **6**: 521–526.
17. Hoshino M, Imamura M, Ikehara K, Hama Y. *J. Phys. Chem.* 1981; **85**: 1820–1823.
18. Alexander HC, Dill DC, Smith LW, Guiney PD, Dorn P. *Bisphenol A* 2000; **1**: 42–50.
19. Kitano H, Endo H, Gemmei-ide M, Kyogoku M. *J. Inclusion Phenom. Mol. Recognit. Chem.* 2003; **47**: 83–90.
20. Kitano H. *Taira Y. Langmuir* 2002; **18**: 5835–5840.
21. Del Olmo M, Zafra A, Gonzales-Casado A, Vilchez JL. *Int. J. Environmental Chem.* 1998; **69**: 99–110.
22. Rekharsky MV, Goldberg RN, Schwarz FP, Tewari YB, Roos PD, Yamashoji Y, Inoue Y. *J. Am. Chem. Soc.* 1995; **117**: 8830–8840.
23. Bertrand GL, Faulkner JR, Han SM, Armstrong DW. *J. Phys. Chem.* 1989; **93**: 6863–6867.
24. Suzuki T. *J. Chem. Inf. Comput. Sci.* 2001; **41**: 1266–1273.
25. Uccello-Barretta G, Balzano F, Paolino D, Ciaccio R, Guccione S. *Bioorg. Med. Chem.* 2005; **13**: 6502–6512.
26. (a) Amato ME, Lombardo GM, Pappalardo GC, Scarlatta G. *J. Mol. Struct.* 1995; **350**: 71–82; (b) Ivanov PM, Jaime C. *J. Mol. Struct.* 1996; **377**: 137–147.
27. Huang M, Watts JD, Bodor N. *Int. J. Quantum Chem.* 1997; **65**: 1135–1152.
28. Rekharsky MV, Inoue Y. *Chem. Rev.* 1998; **98**: 1875–1917.
29. Benesi HA, Hildebrand JH. *J. Am. Chem. Soc.* 1949; **71**: 2703–2707.
30. Inoue Y, Hakushi T, Liu Y, Tong LH, Shen BJ, Jin DS. *J. Am. Chem. Soc.* 1993; **115**: 475–481.
31. Lewis EA, Hansen LD. *J. Chem. Soc., Perkin Trans.* **2***:* 1973; 2081–2085.
32. Tong WQ, Lach JL, Chin TF, Guillory JK. *Pharm. Res.* 1991; **8**: 951–957.
33. Catena GC, Bright FV. *Anal. Chem.* 1989; **61**: 905–909.
34. The hydrophobicities of the four guests were estimated by measurement of contact angles. The surface energies were calculated from the contact angle, and were as follows: BPA (57.1 mN/m), FBPA (32.7 mN/m), BIP (58 mN/m), IPP (56.7 mN/m).
35. Adamson AW, Gast AP. *Physical Chemistry of Surfaces*, 6th Edn. John Wiley: New York, Chichester, Weinheim, 1997.
36. Inoue Y, Hakushi T, Liu Y, Tong L-H, Shen B-J, Jins D-S. *J. Am. Chem. Soc.* 1993; **115**: 475–481.
37. Liu Y, Chen G, Zhang H, Song H, Ding F. *Carbohydr. Res.* 2004; **339**: 1649–1654.
38. Djedaini F, Perly B. *J. Pharm. Sci.* 1991; **80**: 1157–1161.
39. Ivanov PM, Slvatierra D, Jaime C. *J. Org. Chem.* 1996; **61**: 7012–7017.
40. Delpuech JJ. *Dynamics of Solution and Fluid Mixtures by NMR*. Wiley: New York, 1994.
41. Lincoln SF, Hounslow AM, Coates JH, Doddridge BG. *J. Chem. Soc., Faraday Trans.* **1***:* 1987; **83**: 2697–2703.
42. Alderfer JL, Eliseev AV. *J. Org. Chem.* 1997; **62**: 8225–8226.
43. Dodziuk H. *J. Mol. Struct.* 2002; **614**: 33–45.
44. Zhao Y, Truhlar DG. *Phys. Chem. Chem. Phys.* 2005; **7**: 2701–2705.
45. (a) Kinoshita M, Okamato Y, Hirata F. *J. Chem. Phys.* 1997; **107**: 1586–1599; (b) Vath P, Zimmt MB, Matyushov DV, Voth GA. *J. Phys. Chem. B* 1999; **103**: 9130-9140; (c)Matyushov DV, Ladanyi BM. *J. Chem. Phys.* 1999; **110**: 994–1009.
46. Zhao Y, Truhlar DG. *J. Chem. Theory Compt.* 2005; **1**: 415–432.
47. Dewar MJS, Zoebisch EG, Healy E, Stewart JJP. *J. Am. Chem. Soc.* 1985; **107**: 3902–3909.
48. AMPAC 7.0 code, Semichem, Shawnes, KS 66216, USA.
49. (a) Becke AD. *J. Chem. Phys.* 1993; **98**: 5648–5652; (b) Lee C, Yang W, Parr RG. *Phys. Rev. B* 1988; **37**: 785–789.
50. (a) Hariharan PC, Pople JA. *Chem. Phys. Lett.* 1972; **66**: 217–219; (b) Hehre WJ, Radom L, Schleyer PVR, Pople JA. *Ab Initio Molecular Orbital Theory.* Wiley: New York, 1986.
51. Gaussian 98 (Revision A.6), Frisch MJ, Trucks GW, Schlegel HB, Scuseria GE, Robb MA, Cheeseman JR, Zakrzewski VG, Montgomery JA, Stratmann RE, Burant JC, Dapprich S, Millam JM, Daniels AD, Kudin KN, Strain MC, Farkas O, Tomasi J, Barone V, Cossi M, Cammi R, Mennucci B, Pomelli C, Adamo C, Clifford S, Ochterski J, Petersson GA, Ayala PY, Cui Q, Morokuma K, Malick DK, Rabuck AD, Raghavachari K, Foresman JB, Cioslowski J, Ortiz JV, Stefanov BB, Liu G, Liashenko A, Piskorz P, Komaromi I, Gomperts R, Martin RL, Fox DJ, Keith T, Al-Laham MA, Peng CY, Nanayakkara A, Gonzalez C, Challacombe M, Gill PMW, Johnson BG, Chen W, Wong MW, Andres JL, Head-Gordon M, Replogle ES, Pople JA. Gaussian, Inc.: Pittsburgh, PA, 1998.
52. Ditchfield R. *Mol. Phys.* 1974; **27**: 789–807.
53. Botsi A, Yannakopoulou K, Hadjoudis E, Waite J. *Carbohydrate Res.* 1996; **283**: 1–16.
54. Stewart JJP*J. Comput. Chem.* 1989; **10**: 209–220.
55. Metzger TG, Ferguson DM, Glauser WA. *J. Comp. Chem.* 1997; **18**: 70–79.
56. Betzel C, Saenger W, Hingerty BE, Brown GM. *J. Am. Chem. Soc.* 1984; **106**: 7545–7557.
57. (a)Klamt A, Schürmann G. *J. Chem. Soc., Perkin Trans.* **2***:* 1993; **5**: 799–805; (b) Klamt A. *J. Phys. Chem.* 1995; **99**: 2224–2235.
58. Sim F, St Amant A, Papai I, Salahub DR. *J. Am. Chem. Soc.* 1992; **114**: 4391–4000.
59. (a) Kristyan S, Pulay P. *Chem. Phys. Lett.* 1994; **229**: 175–180; (b) Hobza P, Sponer J, Reschel TJ. *Comput. Chem.* 1995; **16**: 1315–1325; (c) Ruiz E, Salahub DR, Vela A. *J. Phys. Chem.* 1996; **100**: 12265–12276.
60. Zhao Yan, Truhlar DG. *J. Chem. Theory Comput.* 2005; **1**: 415–432.

DOI: 10.1002/poc